Journal of Applied Polymer Science

Gelation and crosslinking characteristics of photopolymerized poly(ethylene glycol) hydrogels

Ji Won Hwang,[1] Seung Man Noh,[2] Bumsang Kim,[3] Hyun Wook Jung[1]

[1]Department of Chemical and Biological Engineering, Korea University, Seoul 136-713, Republic of Korea
[2]Research Center for Green Fine Chemicals, Korea Research Institute of Chemical Technology, Ulsan 681-310, Republic of Korea
[3]Department of Chemical Engineering, Hongik University, Seoul 121-791, Republic of Korea
Correspondence to: B. Kim (E-mail: bskim@hongik.ac.kr) and H. W. Jung (E-mail: hwjung@grtrkr.korea.ac.kr)

ABSTRACT: The gelation and crosslinking features of poly(ethylene glycol) (PEG) hydrogels were scrutinized through the UV polymerization processes of poly(ethylene glycol) methacrylate (PEGMA) and poly(ethylene glycol) dimethacrylate (PEGDMA) mixtures. The real-time evolutions of the elastic moduli of the prepolymerized mixtures with different crosslinking ratios of PEGMA and PEGDMA and the photoinitiator concentrations were measured during photopolymerization. The rheological properties were compared with other properties of the PEG hydrogels, including the relative changes in the C=C amounts in the mixtures before and after UV irradiation, water swelling ratio, gel fraction, mesh size, and mechanical hardness. As the portion of PEGDMA as a crosslinker increased, the final elastic modulus and gel fraction increased, whereas the swelling ratio and scratch penetration depth at the hydrogel film surface decreased because of the formation of compact networks inside the hydrogels. These results indicate that there was a good correlation between the rheological analysis for predicting the crosslinking transition during photopolymerization and the macroscopic properties of the crosslinked hydrogels. © 2015 Wiley Periodicals, Inc. J. Appl. Polym. Sci. **2015**, *132*, 41939.

KEYWORDS: photopolymerization; rheology; swelling; viscosity and viscoelasticity

Received 4 August 2014; accepted 3 January 2015
DOI: 10.1002/app.41939

INTRODUCTION

Hydrogels are three-dimensional polymer networks that are capable of absorbing large amounts of water or aqueous solvent yet are insoluble because of the presence of crosslinks, entanglements, or crystalline regions. Hydrogels have been very useful in biomedical and pharmaceutical applications because of their high water content and rubbery nature, which are quite analogous to natural tissues and their biocompatibility.[1–5] Poly(ethylene glycol) (PEG) plays a key role in the production of attractive hydrogels for many promising applications, including tissue engineering, drug-delivery devices, biosensors, bioseparations, and antifouling membranes because of its fascinating features. PEG (1) is biocompatible; (2) makes drugs with low solubility soluble; (3) serves to hide the circulating drug system from immune recognition, especially in the liver; (4) provides protein- and cell-resistant properties to material surfaces containing PEGs; (5) does not interact severely with blood and cellular proteins; and (6) is naturally excreted by the body under low-molecular-weight conditions.[6–13]

The final mechanical properties and structural morphology of hydrogels, determined during the polymerization process, called the *gelation process*, are very important factors for their specific biorelated applications. For example, the mesh size of the hydrogels in drug-delivery systems or electrophoresis gels and the mechanical properties of the hydrogels as antifouling coating materials on the membranes or bone-regeneration scaffolds play important roles.[14–16] However, these are still considered secondary requirements and are overlooked in favor of more biological-based analysis. Also, the rheological properties, including the elastic and viscous moduli (G' and G'', respectively), can noticeably portray the crosslinking formation as the gelation evolves from liquidlike to solidlike phases, by offering a correlation between the reaction kinetics and the mechanical and morphological features of the final crosslinked samples. Moreover, rheological investigation during polymerization can give useful information on the formation of the hydrogel network in real time.[17–19]

The aim of this study was to investigate the effects of the percentage of ingredients in prepolymerized mixtures on the gelation process through the monitoring of the *in situ* rheological evolution of the PEG hydrogels during UV polymerization to optimally tailor the hydrogels for the specific requirements of the

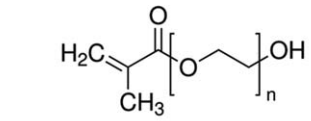

Poly(ethylene glycol) methacrylate (PEGMA)

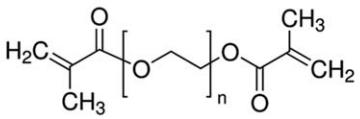

Poly(ethylene glycol) dimethacrylate (PEGDMA)

Figure 1. Chemical structures of PEGMA and PEGDMA.

application. To produce the PEG hydrogels, free-radical photopolymerization is one of the most representative techniques for fabricating biomaterials that afford many advantages, including relatively high reaction rates at room temperature, spatial and temporal control of the initiation process, low energy input, and chemical versatility. *In situ* rheological tests under small-amplitude oscillatory shear (SAOS) mode have been carried out during photopolymerization for PEG hydrogels. We focused mainly on the use of a rotational rheometer with an integrated UV illumination module and the influence of the concentrations of the monomer [poly(ethylene glycol) methacrylate (PEGMA)], crosslinker [poly(ethylene glycol) dimethacrylate (PEGDMA)], and photoinitiator (Irgacure 184) on the temporal changes of the rheological properties during the gelation process and mechanical responses of the resulting hydrogel networks. A simplified model from the classical rubber elasticity theory[20,21] was then used to estimate the average gel mesh size of the hydrogels on the basis of their water swelling ratio. In addition, the real mechanical properties of the photopolymerized hydrogel films were figured out from the scratch patterns over the film surface by means of a nano scratch test (NST).[22,23]

EXPERIMENTAL

PEG Hydrogel Formulations

The prepolymerized mixtures were prepared by the combination of various amounts of PEGMA (molecular weight = 360) as a monomer, PEGDMA (molecular weight = 330) as a crosslinker, and 1-hydroxycyclohexyl phenyl ketone (known as Irgacure 184) as a photoinitiator. PEGMA and PEGDMA (Figure 1) were purchased from Sigma-Aldrich. Irgacure 184 was obtained from BASF Schweiz AG (Switzerland).

To determine the effect of the reaction conditions, including the molar ratio between the monomer and crosslinker (crosslinking ratio) and the photoinitiator concentration, on the gelation process and mechanical responses of the resulting hydrogel networks, various PEG hydrogel samples with different formulations were prepared, as listed in Table I.

Table I. Compositions of PEGMA and PEGDMA in the Prepolymerized Mixtures

	Weight fraction (wt %)		Molar ratio
Sample	PEGMA (monomer)	PEGDMA (crosslinker)	PEGMA /PEGDMA
C0.5	68.5	31.5	1 : 0.5
C1.0	52.2	47.8	1 : 1
C2.0	35.3	64.7	1 : 2

Characterization Methods

Real-Time Rheological Measurements During Photopolymerization. The polymerization kinetics of the PEG hydrogels could be effectively interpreted from their real-time rheological properties, as measured by a rotational rheometer (MCR-301, Anton Paar, Austria) with a UV module. In previous studies,[20,23–29] it was successfully confirmed that the rheological data suitably reflected the *in situ* polymerization, gelation, and curing features of polymeric materials. Under SAOS mode, the evolution of G' was acquired during the UV polymerization. The rheological properties of the hydrogels considered in this study were measured under the same temperature and UV irradiation conditions to quantitatively compare the microstructural progress inside them and connected with the formation of the crosslinked network. The level of the crosslinked network estimated from G' allowed us to understand the network structures of the polymerized hydrogels. As depicted in Figure 2, the ambient temperature around the samples was manipulated by the convection of heating of cooling the air in the controlled temperature chamber. The oscillatory shear was applied to parallel plates 8 mm in diameter with a 2% strain; this guaranteed the linear viscoelasticity regime during the rheological measurement. The gap between the two plates was 300 μm. The input frequency during the SAOS test was set to 5 Hz because of the fast UV polymerization. The samples were polymerized under the same energy density of UV irradiation penetrating below

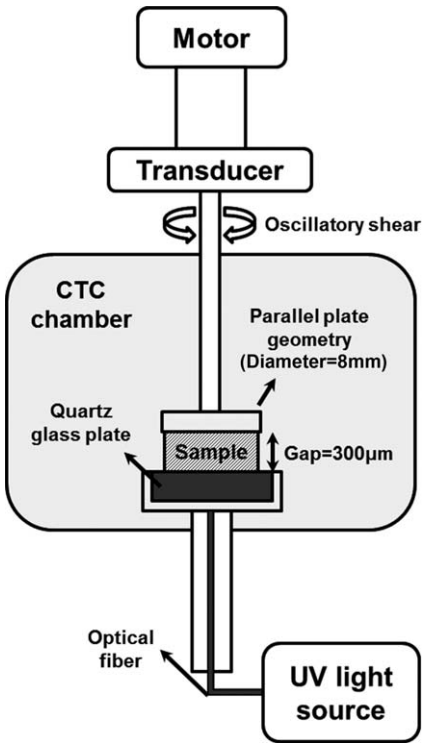

Figure 2. Schematic geometry of the rotational rheometer equipped with a UV module and a heating/cooling chamber.

the glass substrate. Note that the intensity of the UV source used in our study was measured at certain wavelengths because of the broad distribution of its wavelength: 2.83 mW/cm^2 for the wavelength of 365 nm or 0.698 mW/cm^2 for the wavelength of 313 nm.

Fourier Transform Infrared (FTIR) Analysis. The chemical reaction involving the C═C double bonds in the methacrylate of PEGMA and PEGDMA was analyzed by the monitoring of the disappearance of the IR band at 1637 cm^{-1}. The absorbance peaks were obtained via attenuated total reflectance–FTIR spectroscopy (Spectrum 100, PerkinElmer). The conversion of the C═C groups was evaluated through a comparison of the difference in the absorbance peaks at 1637 cm^{-1} before and after the UV dose.

Swelling Ratio and Gel Fraction Measurements. To determine the water swelling behavior of the hydrogels, the disk-shaped hydrogel films obtained from the rheological tests were dried in a vacuum oven for 24 h at 80°C. They were then weighed and immersed in distilled water at room temperature. After they were fully swollen for over 72 h, the films were taken out from the water and then weighed again. The water swelling of the hydrogels was expressed as the weight swelling ratio (q) and was calculated from eq. (1):

$$q = W_s / W_d \quad (1)$$

where W_s and W_d are the weight of the swollen hydrogel and the weight of the dried one before swelling, respectively. The equilibrium weight swelling ratio was calculated when the weight of the swollen hydrogel reached a constant value.

The gel fraction of the hydrogel (f) was further evaluated by the complete drying of the swollen hydrogel for 24 h at 80°C to extract the unreacted parts inside them on the basis of the following equation:

$$f(\%) = W_{ex} / W_d \times 100 \quad (2)$$

where W_{ex} is the dried weight of the hydrogel after the extraction of soluble parts.

Mesh Size Calculation. The mesh size (ξ) could be predicted from the molecular weight between two crosslinking points (M_c) and from the swelling experiment as follows:[20,21]

$$M_c = \frac{n(\text{PEGMA})}{n(\text{PEGDMA})} M(\text{PEGMA}) + M(\text{PEGDMA}) \quad (3)$$

$$\xi = l\left(\frac{2M_c}{\bar{M}}\right) C_N^{1/2} q^{1/3} \quad (4)$$

where M(PEGMA) is the molecular weight of PEGMA (360 g/mol); M(PEGDMA) is the molecular weight of PEGDMA (330 g/mol); n(PEGMA) and n(PEGDMA) are the moles of PEGMA and PEGDMA used in the experiments, respectively; l is the length of a C—C single bond (l = 0.154 nm); $\bar{M}$ is the average molecular weight of PEGMA and PEGDMA considering their ratio in the gel composition; C_N is the characteristic ratio (C_N for acrylates = 6.9);[30–33] and q is the swelling ratio defined in eq. (1).

NST. NST (open platform, CSM Instruments, Switzerland) is the method for the measurement of the mechanical resistance of hydrogel films through the imposition of a progressive deformation load on the film surface.[22,23] During this test, the normal force acting on the surface of the hydrogel films is gradually increased from 0.5 to 18 mN with a scanning load speed of 1 mm/min. A spheroconical 90° nanoindenter probe with an indenter radius of 0.5 μm checked the scratch depths (penetration depth) of each sample according to ASTM D 7187. The thickness of the crosslinked hydrogel films made during the rheological tests was about 300 μm.

RESULTS AND DISCUSSION

Conversion of Methacrylate Bonds in the PEG Hydrogels via FTIR Analysis

The IR absorbances of the samples before and after UV polymerization were measured to qualitatively investigate the conversion of C═C bonds in the methacrylate groups of both PEGMA and PEGDMA. Figure 3 presents the peaks of IR vibrations of the methacrylate double bond at 1637 cm^{-1} compared to those of the unreacted groups at 2870 cm^{-1}. That is, the FTIR spectra in

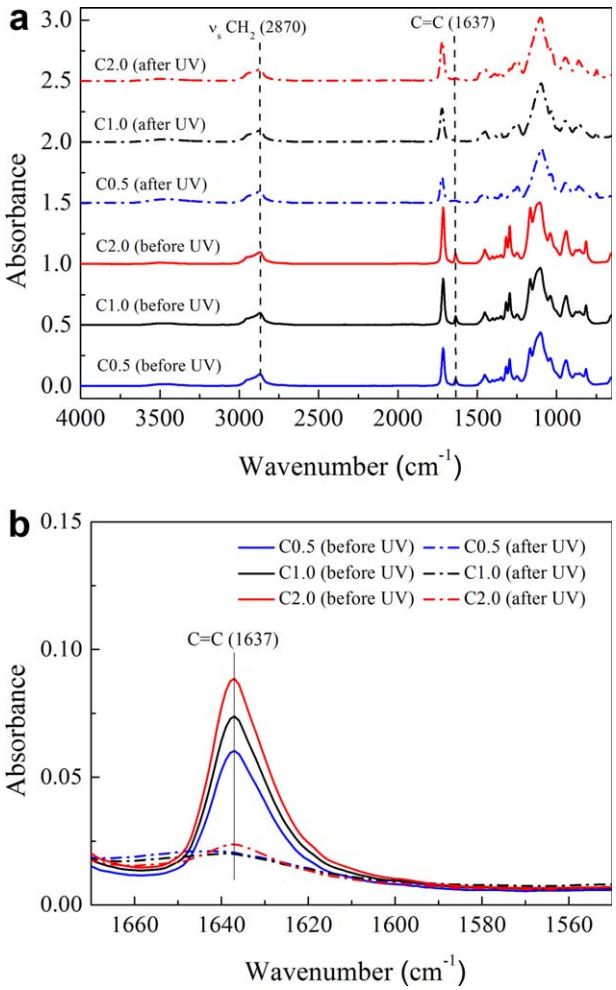

Figure 3. FTIR data for the PEG hydrogels before and after UV polymerization: the effect of the crosslinking ratio with a photoinitiator at 1 wt % (a) in the wave-number range 650–4000 cm^{-1} and (b) near the wave number 1637 cm^{-1}. [Color figure can be viewed in the online issue, which is available at wileyonlinelibrary.com.]

all cases contained symmetric methylene stretching ($\nu_s CH_2$) at 2870 cm^{-1}, which did not participate in the polymerization, and C═C double bonds in the methacrylate groups of PEGMA and PEGDMA, which participated in the polymerization [Figure 3(a)]. As shown in Figure 3(b), the heights of the solid line peaks and the dash–dot line peaks denoted the relative amounts of C═C bonds before and after the polymerization, respectively. Because the C0.5, C1.0, and C2.0 samples were prepared with different crosslinking ratios of 1 : 0.5, 1 : 1, and 1 : 2, respectively, the C2.0 sample had the largest number of C═C bonds in the PEGMA–PEGDMA mixtures before polymerization; this resulted in the highest absorbance peak in the spectra. After the UV polymerization, the absorbance peaks at 1637 cm^{-1} disappeared because of the conversion of C═C bonds into C—C bonds. These results show that the PEGMA–PEGDMA mixtures developed the crosslinked structure by free-radical UV polymerization and finally formed PEG hydrogel networks. The effect of the photoinitiator content on the conversion of C═C bonds by UV polymerization is illustrated in Figure 4. Before the polymerization, the initial heights of all of the C1.0 samples with different portions of photoinitiator were exactly the same because they included an equivalent number of moles of monomer and crosslinker. After the polymerization, the spectra of Figure 4 show that the peaks of the C═C bonds in all of the samples vanished; this demonstrated that most of the reactants were reacted. We also found that there was no significant effect of the photoinitiator concentration (at least >0.5 wt %) on the complete conversion of C═C bonds in the PEGMA–PEGDMA mixtures. These results indicate that the crosslinked networks of the PEG hydrogels could be achieved with the free-radical photopolymerization carried out in this study.

Rheological Behavior of the Hydrogels During the Photopolymerization Process

To examine the effect of the ingredient composition on the polymerization kinetics and crosslinking formation of the PEG hydrogel, the real-time rheological properties (G' here) of the PEGMA–PEGDMA mixtures were systematically measured during the UV polymerization process by a rotational rheometer; this directly identified the development of the hydrogel network structures. Note that the elasticity of the PEGMA–PEGDMA mixtures without UV irradiance could not be detected because of their Newtonian fluid characteristics. The

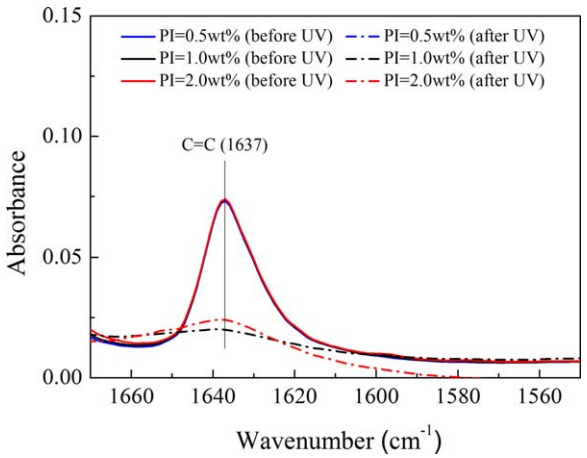

Figure 4. FTIR data for the PEG hydrogels before and after UV polymerization: the effect of the photoinitiator (PI) concentration for the C1.0 sample near the wave number 1637 cm^{-1}. [Color figure can be viewed in the online issue, which is available at wileyonlinelibrary.com.]

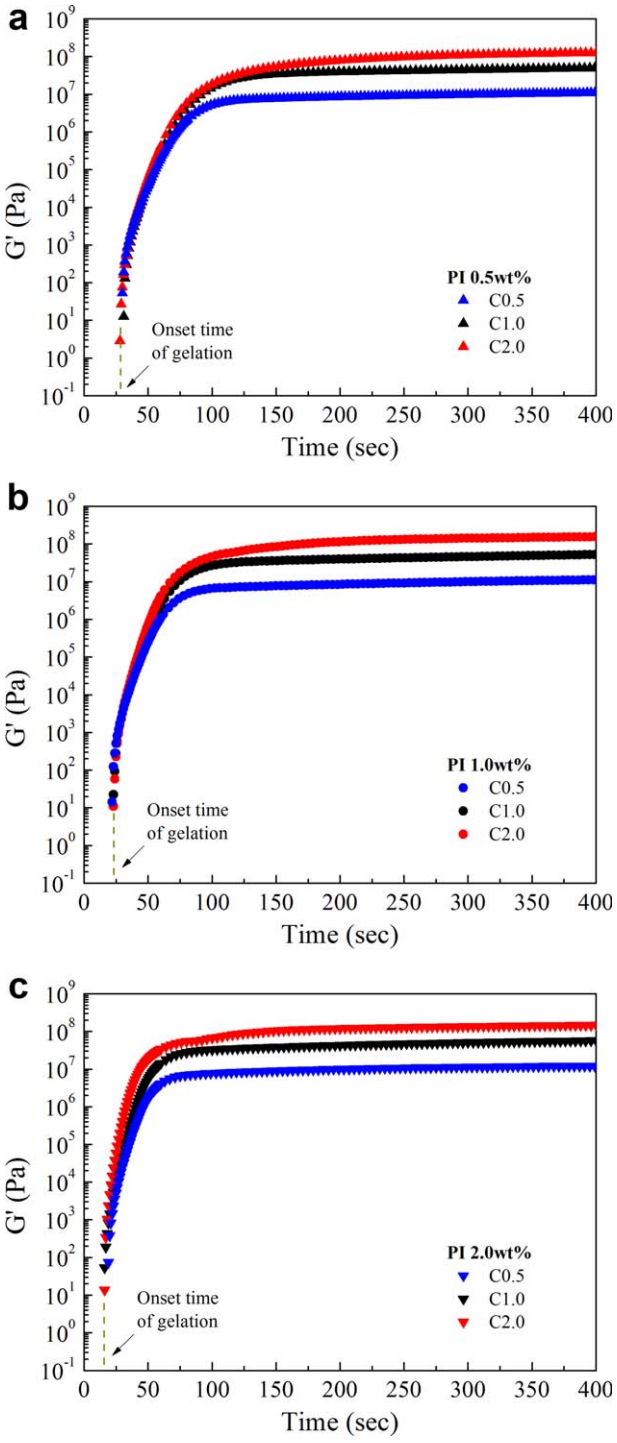

Figure 5. Effect of the crosslinking ratio and photoinitiator concentration on G' during UV polymerization for samples with (a) 0.5, (b) 1.0, and (c) 2.0 wt % PI. [Color figure can be viewed in the online issue, which is available at wileyonlinelibrary.com.]

Table II. Onset Times of Gelation for the PEG Hydrogel Samples with Different Photoinitiator Concentrations in the Rheological Tests

	Onset time of gelation (s)		
Content of the photoinitiator (wt %)	C0.5	C1.0	C2.0
0.5	29	31	27
1	21	23	22
2	18	15	15

basic shear viscosities of the unreacted samples at room temperature were 0.0321 Pa s for C0.5, 0.0246 Pa s for C1.0, and 0.0202 Pa s for C2.0, respectively.

The effects of the crosslinking ratio and photoinitiator concentration on the rheological evolution during the photopolymerization process are shown in Figure 5. As the crosslinking ratio increased (from 1 : 0.5 to 1 : 2), the final G' at the plateau increased. This was because the C2.0 sample, which contained the largest amount of PEGDMA with double bonds at both ends, notably promoted the densest crosslinked network after the polymerization; this agreed with the results of the FTIR spectra shown in Figure 3.

The *onset time of gelation*, defined as the time when the promotion of G' was first triggered from zero value (see Figure 5), is listed in Table II as a function of the crosslinking ratio and photoinitiator concentration. As the photoinitiator concentration increased, the onset of gelation and UV irradiation time needed to reach the final G' decreased. This was because the free radicals that initiated the polymerization were more activated with the photoinitiator concentration, and this led to the rapid initiation of polymerization and the completion of network formation. However, there was not much difference in the final G' values according to the photoinitiator concentration; this was similar to the FTIR results.

Swelling Ratio and Gel Fraction of the PEG Hydrogels

The rheological data in the previous section supported the microscopic aspects of the crosslinking formation of the hydrogels. Thus, to consider macroscopic perspectives, the water swelling ratios of the photopolymerized PEG hydrogel films made via SAOS tests under different crosslinking ratios and photoinitiator concentration conditions were determined. As shown in Figure 6(a), the PEG hydrogel with a higher crosslinking ratio exhibited a lower swelling ratio because of the denser crosslinking formation. However, there was no considerable effect of the photoinitiator content on the swelling ratio of the hydrogels. The mesh size of the PEG hydrogels predicted from eq. (4) decreased as the crosslinking ratio increased. The mesh sizes of the C0.5, C1.0, and C2.0 samples were 1.089, 0.866, and 0.733 nm, respectively. The gel fraction could also be used as a quantitative indicator for the efficiency of network formation.[34] As the crosslinking ratio increased, the gel fraction of the hydrogels increased [Figure 6(b)]; this substantiated that more gelation occurred through the formation of more crosslinking networks in the sample with a higher crosslinking ratio.

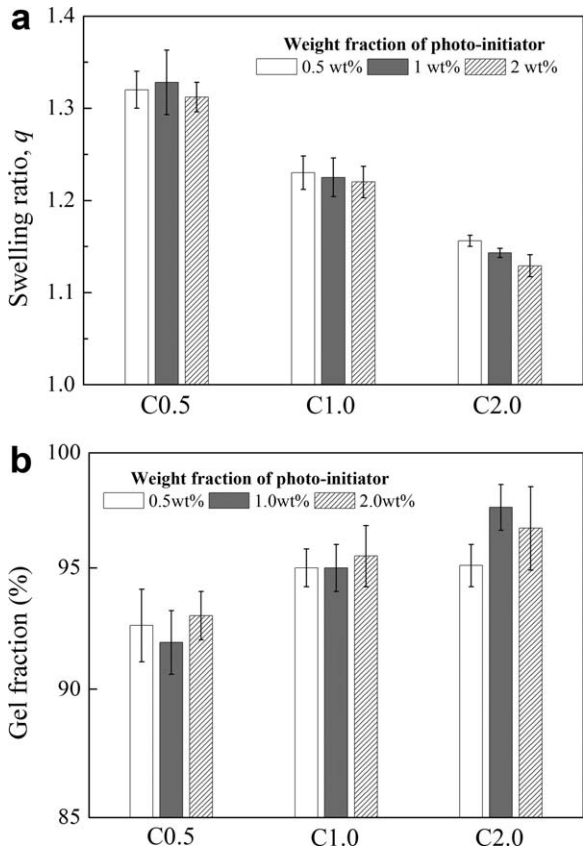

Figure 6. (a) Water swelling ratio and (b) gel fraction of the PEG hydrogels as functions of the crosslinking ratio and photoinitiator concentration.

Mechanical Hardness of the PEG Hydrogel Films

Because the swelling properties did not represent the real macroscopic mechanical properties of the PEG hydrogels, the mechanical hardness of the PEG hydrogel films after rheological tests were compared by the measurement of scratches on the film surfaces in NST. Figure 7 displays the patterns of the penetration depth along a 0.9 mm long scratch by the gradual imposition oof the vertical load from 0.5 to 18 mN at the surface of several hydrogel films. The penetration depth profiles were closely linked

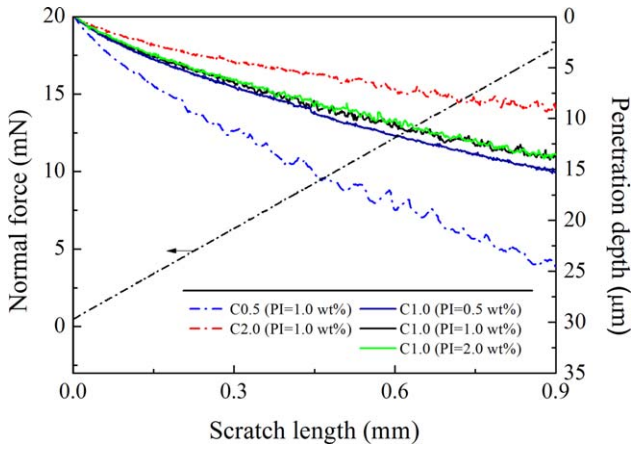

Figure 7. Penetration depth profiles for the PEG hydrogel films through NST. [Color figure can be viewed in the online issue, which is available at wileyonlinelibrary.com.]

with the hardness of the films. It was expected that hard films would be less damaged than soft ones, and this would result in a shallow penetration depth. As shown in Figure 7, the penetration depth was inversely related to the concentration of the crosslinker. In other words, the C2.0 sample showed the shallowest penetration depth with the same photoinitiator content; this proved very high mechanical properties. This was surely due to the high level of the crosslinking formation for C2.0 with a large number of C═C double bonds to be converted to C—C bonds. We also revealed that the difference in the penetration depth for the C1.0 samples with different portions of photoinitiator over 0.5 wt % was insignificant. The trends of the mechanical property data were well-matched with those from FTIR spectroscopy, rheology, swelling ratio, and gel fraction measurements.

CONCLUSIONS

From the prepolymerized mixtures of PEGMA and PEGDMA with different crosslinking ratios and photoinitiator concentrations, crosslinked PEG hydrogels were prepared by means of a UV polymerization process. The conversion of C═C of the methacrylate groups in the PEG hydrogels by photopolymerization was confirmed from FTIR analysis. The gelation and crosslinking features for the PEG hydrogels were predicted by real-time rheological data during polymerization. From the evolution of the rheological G' data, the onsets of gelation and final modulus values for various PEG hydrogels could be clearly discerned. The increased crosslinking ratio caused the final G' and gel fraction to increase, whereas the water swelling ratio and scratch penetration depth decreased because of the formation of an enhanced crosslinked network inside PEG hydrogels. These results indicate that the properties of the final crosslinked hydrogels, including the water swelling ratio, gel fraction, and scratch penetration depth, were effectively tuned by comparison with the reaction conversion via free-radical polymerization and the *in situ* rheological data.

ACKNOWLEDGMENTS

This study was supported by research grants from the Human Resources Development Program of the Korea Institute of Energy Technology Evaluation and Planning (contract grant number 20134010200600), the Basic Science Research Program through the National Research Foundation of Korea (contract grant number NRF-2012R1A1A2004659), and the Hongik University Research Fund.

REFERENCES

1. Langer, R.; Peppas, N. A. *AIChE J.* **2003**, *49*, 2990.
2. Peppas, N. A.; Bures, P.; Leobandung, W.; Ichikawa, H. *Eur. J. Pharm. Biopharm.* **2000**, *50*, 27.
3. Nguyen, K. T.; West, J. L. *Biomaterials* **2002**, *23*, 4307.
4. Chaturvedi, K.; Ganguly, K.; Nadagouda, M. N.; Aminabhavi, T. M. *J. Controlled Release* **2013**, *165*, 129.
5. Lee, S. C.; Kwon, I. K.; Park, K. *Adv. Drug Delivery Rev.* **2013**, *65*, 17.
6. Suggs, L. J.; Shive, M. S.; Garcia, C. A.; Anderson, J. M.; Mikos, A. G. *J. Biomed. Mater. Res. A* **1999**, *46*, 22.
7. Bryant, S. J.; Anseth, K. S. *J. Biomed. Mater. Res. A* **2002**, *59*, 63.
8. Lin, G.; Tarasevich, B. *J. Appl. Polym. Sci.* **2013**, *128*, 3534.
9. Ikeda, Y.; Katamachi, J.; Kawasaki, H.; Nagasaki, Y. *Bioconjugate Chem.* **2013**, *24*, 1824.
10. Tan, G.; Liao, J.; Ning, C.; Zhang, L. *J. Appl. Polym. Sci.* **2012**, *125*, 3509.
11. Hood, R. R.; Shao, C. R.; Omiatek, D. M.; Vreeland, W. N.; DeVoe, D. L. *Pharm. Res.* **2013**, *30*, 1597.
12. Roach, P.; McGarvey, D. J.; Lees, M. R.; Hoskins, C. *Int. J. Mol. Sci.* **2013**, *14*, 8585.
13. Kiuchi, H.; Kai, W.; Inoue, Y. *J. Appl. Polym. Sci.* **2008**, *107*, 3823.
14. Killion, J. A.; Geever, L. M.; Devine, D. M.; Kennedy, J. E.; Higginbotham, C. L. *J. Mech. Behav. Biomed. Mater. A* **2011**, *4*, 1219.
15. Ju, H.; McCloskey, B. D.; Sagle, A. C.; Wu, Y.-H.; Kusuma, V. A.; Freeman, B. D. *J. Membr. Sci.* **2008**, *307*, 260.
16. Wang, J.; Ugaz, V. M. *Electrophoresis* **2006**, *27*, 3349.
17. Buwalda, S. J.; Calucci, L.; Forte, C.; Dijkstra, P. J.; Feijen, J. *Polymer* **2012**, *53*, 2809.
18. Censi, R.; Fieten, P. J.; di Martino, P.; Hennink, W. E.; Vermonden, T. *Macromolecules* **2010**, *43*, 5771.
19. Bader, R. A.; Rochefort, W. E. *J. Biomed. Mater. Res. A* **2008**, *86*, 494.
20. Adrus, N.; Ulbricht, M. *React. Funct. Polym.* **2013**, *73*, 141.
21. Ju, H.; McCloskey, B. D.; Sagle, A. C.; Kusuma, V. A.; Freeman, B. D. *J. Membr. Sci.* **2009**, *330*, 180.
22. Consiglio, R.; Randall, N. X.; Bellaton, B.; Stebut, J. V. *Thin Solid Films* **1998**, *332*, 151.
23. Noh, S. M.; Lee, J. W.; Nam, J. H.; Byun, K. H.; Park, J. M.; Jung, H. W. *Prog. Org. Coat.* **2012**, *74*, 257.
24. Chiou, B. S.; English, R. J.; Khan, S. A. *Macromolecules* **1996**, *29*, 5368.
25. Calvet, D.; Wong, J. Y.; Giasson, S. *Macromolecules* **2004**, *37*, 7762.
26. Hwang, J. W.; Kim, K. N.; Lee, G. S.; Nam, J. H.; Noh, S. M.; Jung, H. W. *Prog. Org. Coat.* **2013**, *76*, 1666.
27. Zhou, C.; Wu, Q.; Zhang, Q. *Colloid Polym. Sci.* **2011**, *289*, 247.
28. Bonino, C. A.; Samorezov, J. E.; Jeon, O.; Alsberg, E.; Khan, S. A. *Soft Matter* **2011**, *7*, 11510.
29. Park, S.; Hwang, J. W.; Kim, K. N.; Lee, G. S.; Nam, J. H.; Noh, S. M.; Jung, H. W. *Korea–Aust. Rheol. J.* **2014**, *26*, 159.
30. Flory, P. J.; Rehner, J. *J. Chem. Phys.* **1943**, *11*, 512.
31. Flory, P. J. Statistical Mechanics of Chain Molecules; Interscience: New York, **1969**.
32. Peppas, N. A.; Moynihan, H. J.; Lucht, L. M. *J. Biomed. Mater. Res. A* **1985**, *19*, 397.
33. Fanger, C.; Wack, H.; Ulbricht, M. *Macromol. Biosci.* **2006**, *6*, 393.
34. Wu, Y.-H.; Park, H. B.; Kai, T.; Freeman, B. D.; Kalika, D. S. *J. Membr. Sci.* **2010**, *347*, 197.